Effective Structural System for the Affordable Housing Construction

Prof. Mostafa Hasan Kotb[1], Prof. Amin Saleh Aly[2], Eng. Khaled Muhammad Ali Muhammad[3]

[1]*Professor, Civil Engineering Dep., Structural Engineering Dept., Faculty of Engineering, Al-Azhar Univ., Cairo, Egypt*
[2]*Professor, Civil Engineering Dep., Structural Engineering Dept., Faculty of Engineering, Ain Shams Univ., Cairo, Egypt*
[3]*Ph.D. Student, Civil Engineering Dep., Structural Engineering Dept., Faculty of Engineering, Al-Azhar Univ., Cairo, Egypt*

Abstract: **Design of ferroconcrete structures is ruled by the nonlinear manner of concrete and by its completely different strengths in tension and compression. The aim of this text is to show a computational process for optimum theoretical design of reinforced concrete structures, supported topology optimization with elastic-plastic material modeling. Concrete and steel are both considered as elastic-plastic materials, also the acceptable yield criteria and post-yielding response. The same process is applied also for topology optimization of alternative material compositions where nonlinear response should be considered. Optimized distribution of material is achieved by introducing interpolation rules for the each; elastic and plastic material properties. Many numerical models illustrate the capability and potential of the planned process.**

Keywords: **Optimization, Structural analysis, Topology design, Plasticity, Reinforced concrete.**

I. INTRODUCTION

Structural optimization techniques are currently changing into an integral part of the design method and are widely applied, as an example, within the automotive and region industries. So far, optimum design had less impact on ancient structural engineering as practiced within the construction industry. One reason may be the issue in combining numerical optimization tools with models which will accurately represent the advanced behavior of composite materials used by the building industry, like reinforced concrete.

The aim of this text is to present a process procedure that allows optimum design of reinforced concrete structures. The approach will simply be generalized to accommodate alternative mixtures of materials besides steel and concrete. By combining topology optimization with elastic-plastic modeling of the candidate materials, it's attainable to think about not only the various elastic stiffness's of the candidate materials, but also their distinct yield limits and yield criteria.

Till now, the overwhelming majority of studies in structural topology optimization are restricted to elastic material. Elastic modeling is sufficient for deciding the distribution of one or a lot of material phases in a very given domain, but only as long as all material points stay in their elastic stress state. This can be clearly not the case in reinforced concrete, where the concrete part fails underneath comparatively low tension stresses. so nonlinear material modeling is important when aiming at optimum design of RC structures. Many studies are dedicated to topology optimization of elastic-plastic structures, as an example based on the von Mises yield criterion or the Drucker-Prager yield criterion. However, to the most effective of the authors' information, this can be the primary study wherever over one nonlinear candidate material is taken into account. Lately, point in time material optimization was used for improving the performance of fiber reinforced concrete Failure behavior of all candidate materials was considered, however the approach taken is restricted to layered structures and can't offer general layouts as obtained using topology optimization.

One approach to visualizing the inner forces in cracked concrete beams is by an easy truss model introduced by Ritter. The resulting model, wide called the strut-and-tie model, has various applications in analysis and design of RC structures subjected to shear forces or torsion moments. Many researchers proposed to use a truss-like structure resulting from linear elastic topology optimization in order to predict a strut-and-tie model. Consequently, the truss bars underneath tension forces represent the placement of steel reinforcement while the compressed bars represent concrete.

In the current study material nonlinearity of each concrete and steel is considered, and therefore a lot of realistic model is obtained. An interpolation scheme is proposed, specified by dynamical the density, the material properties and also the failure criteria vary between concrete and steel. The results of the optimization method are that the optimum distribution of concrete and steel within a definite domain. So an economical strut-and-tie model is directly obtained.

II. NONLINEAR MATERIAL MODEL AND FINITE ELEMENT ANALYSIS

In this section, I shortly overview the elastic-plastic model used in our study and description the resulting nonlinear finite component problem to be resolved. Later, in Section 5, the affiliation between the topology improvement problem and the nonlinear material model will be made.

The main purpose of this study is to optimize the distribution of 2 materials during a given domain, taking the various nonlinear behavior of each materials under consideration. The most plan is to represent the elastic-plastic response of each materials using one generic yield perform that varies in step with the worth of the design variable. For this purpose, I utilize the Drucker-Prager yield criteria. Certainly selections of material properties, the Drucker-Prager yield perform can model the behavior of materials that are abundant stronger in compression than in tension, like soils, rock or plain concrete. Moreover, the von Mises yield criterion that is wide used for metals (having equal strength in tension and compression) may be seen as a specific case of the Drucker-Prager criterion.

In the following, I show the governing equations of the elastic-plastic model, resulting in the local organic problem to be resolved on a Gauss-point level. I follow classical rate-independent plasticity formulations. The Drucker-Prager yield perform may be expressed as;

$$f(\boldsymbol{\sigma},\kappa)=\sqrt{3J_2}+\alpha(\kappa)I_1-\sigma_y(\kappa)\leq 0$$

Where $\mathbf{J_2}$ is the second invariant of the deviatory stress tensor and $\mathbf{I_1}$is the first invariant of the stress tensor. $\boldsymbol{\alpha}$is a material property and $\boldsymbol{\sigma_y}$is the yield stress in uniaxial tension, both functions of the internal hardening parameter **k** according to some hardening functions. The expression$\sqrt{3J2}$ is usually defined as the von Mises stress or equivalent stress. When $\boldsymbol{\alpha}$= 0, Igain the von Mises yield criteria. Isuppose simple isotropic hardening rules;

$$\alpha(\kappa) = constant \quad \textbf{(1)}$$
$$\sigma_y(\kappa) = \sigma_y^0 + HE\kappa \quad \textbf{(2)}$$

Where $\boldsymbol{\sigma^0_y}$ is the initial uniaxial yield stress, **E** is Young's modulus and **H**is a constant, typically in the order of $\mathbf{10^{-2}}$. The equations**(1)** and **(2)**are not certainly suitable for precise modeling of concrete but do not affect the ability to catch the most important failure in concrete that is failure in tension. I suppose an associative flow rule and a simple relation between the hardening parameter and the rate of the plastic flow;

$$\dot{\epsilon}^{pl} = \dot{\lambda}\frac{\partial f}{\partial \boldsymbol{\sigma}}$$
$$\dot{\kappa} = \dot{\lambda} \tag{3}$$

Where $\dot{\epsilon}^{\mathbf{pl}}$ is the plastic strain tensor and the scalar **λ** is usually referred to as the plastic multiplier. The equation**(3)** does not strictly represent hardening mechanisms in metals. Nevertheless, it is correct enough for the aim of the current study, since post-yielding response of the steel phase should not have an effect on the optimal select of material.

Throughout this article, I follow the framework described by Michalis et al. for nonlinear finite element analysis and adjoin sensitivity analysis, where the elastic-plastic nonlinear analysis is seen as a transient, nonlinear coupled problem. In the coupled process, for every increment **n** in the transient analysis, Idefine the unknowns $\mathbf{u_n}$(displacements) and $\mathbf{v_n}$ (stresses and plastic multipliers) that satisfy the residual equations;

$$\mathbf{R}_n(\mathbf{u}_n,\mathbf{u}_{n-1},\mathbf{v}_n,\mathbf{v}_{n-1})=0$$
$$\mathbf{H}_n(\mathbf{u}_n,\mathbf{u}_{n-1},\mathbf{v}_n,\mathbf{v}_{n-1})=0 \tag{4}$$

Where $\mathbf{R_n}$ = 0 is satisfied at the global level and $\mathbf{H_n}$ = 0 is satisfied at each Gauss point. The transient, coupled and nonlinear system of equations is uncoupled by treating the response **v** as a function of the response **u**. When solving the residual equations for the **n-th** "time" increment, the responses $\mathbf{u_{n-1}}$ and $\mathbf{v_{n-1}}$ are known from the previous converged increment. The independent response $\mathbf{u_n}$ is found by an iterative prediction correction procedure in the global level, while for each iterative step the dependent response $\mathbf{v_n(u_n)}$ is found by an inner iterative loop. The responses $\mathbf{u_n}$ and its dependent $\mathbf{v_n}$ are corrected until Eq. **(4)** is stashed to sufficient accuracy. This procedure is repeated for all **N** increments.

Neglecting body forces, $\mathbf{R_n}$ is defined as the difference between external and internal forces and depends explicitly only on $\mathbf{v_n}$.

$$\mathbf{R}_n(\mathbf{v}_n)=\mathbf{f}_n-\int_V \mathbf{B}^T\boldsymbol{\sigma}_n dV$$

Where **B** is the standard strain displacement matrix in the context of finite element procedures. The internal, Gauss-point level variables $\mathbf{v_n}$ are defined as;

$$\mathbf{v}_n=\begin{bmatrix}\boldsymbol{\sigma}_n\\ \lambda_n\end{bmatrix}$$

Where $\boldsymbol{\sigma_n}$ are the stresses and $\boldsymbol{\lambda_n}$ is the plastic multiplier. Furthermore, the residual $\mathbf{H_n}$ is defined as the collection of 2 incremental residuals;

$$\mathrm{H}_n(\mathrm{u}_n,\mathrm{u}_{n-1},\mathrm{v}_n,\mathrm{v}_{n-1})=\begin{bmatrix}\mathrm{Bu}_n-\mathrm{Bu}_{n-1}-\mathrm{D}^{-1}(\boldsymbol{\sigma}_n-\boldsymbol{\sigma}_{n-1})-\frac{\partial f}{\partial \boldsymbol{\sigma}_n}(\lambda_n-\lambda_{n-1})\\ \sqrt{3J_2}+\alpha I_1-\sigma_y(\lambda_n)\end{bmatrix}=\mathbf{0} \tag{5}$$

Here, the primary equation equates total, elastic and plastic strains and also the second represents the need that in plastic response the stress state satisfies the yield condition. Just in case an elastic step is expected by the trial state, then no plastic flow happens and $\boldsymbol{\lambda_n}$= $\boldsymbol{\lambda_{n-1}}$. Thus the primary equation is satisfied trivially by the elastic stress-strain relationship and also the second equation will be forgotten.

The elastic-plastic problem is path-dependent naturally, which means that the evolution of plastic strains underneath a particular load intensity depends on the history of plastic straining and can't be computed properly in one load stage. In observe, this suggests that the **FE** analysis should be resolved incrementally. The default choice for many nonlinear **FE** solvers is to use load management, which means that the whole load is split into a particular variety of increments.

Then for every increment, this stress and strain states are needed for the solution of the local elastic-plastic problem equivalent to following load step. In some cases, it's helpful to modify to displacement management, for example once a tiny low addition to the load causes an oversized extra displacement or once limit points are encountered. Within the context of optimum design, a fixed load intensity throughout the optimization method might cause difficulties in resolution the nonlinear analysis equations for intermediate designs that are terribly versatile.

From this point of view, using displacement management for the nonlinear analysis is preferred. This suggests that the displacement at a specific degree of freedom is prescribed to a particular value for all style cycles. Selecting an acceptable price is possible if the designer has some information relating to the expected deformation, and may even be seen as the simplest way of imposing a needed detection at a particular purpose. Displacement management was used additionally in previous studies relating to topology optimization of elastic-plastic structures.

For these reasons I chiefly use displacement management and corresponding objective functions during this study. Then the worldwide residual equation **(4)** takes the form;

$$\mathbf{R}_n(\mathbf{v}_n, \theta_n) = \theta_n \hat{\mathbf{f}} - \int_V \mathbf{B}^T \boldsymbol{\sigma}_n dV$$

Where $\boldsymbol{\theta_n}$ is the (unknown) load factor in the **n-th** increment and **f** is a constant reference load vector with non-zero entries only at loaded degrees of freedom. When solving the combined equation system for each increment, a single displacement has a prescribed value and the rest, as well as the corresponding load factor $\boldsymbol{\theta_n}$, are specified from equilibrium.

III. PROBLEM FORMULATION

For the aim of optimizing the layout of reinforced concrete structures, I follow the material distribution process for topological design together with the SIMP (Solid Isotropic Material with Penalization) interpolation scheme. The master idea is to interpolate the nonlinear behavior of the 2 candidate materials using the density variables from the topology optimization problem. The interpolation of the elastic modulus is identical to that utilized in standard, linear elastic topology optimization;

$$E(\rho_e) = E_{min} + (E_{max} - E_{min})\rho_e^{p_E}$$

Where $\boldsymbol{\rho_e}$ is the density design variable symmetrical to a specific finite element $\boldsymbol{e}$. Interpolation of the nonlinear response is achieved by adding a dependency on the design variable $\boldsymbol{\rho}$ to the yield function.

$$f(\boldsymbol{\sigma}, \lambda, \rho_e) = \sqrt{3J_2} + \alpha(\rho_e)I_1 - \sigma_y(\lambda, \rho_e) \quad (6)$$

Following a SIMP type process, the interpolating functions $\boldsymbol{\alpha(\rho_e)}$ and $\boldsymbol{\sigma_y(\rho_e)}$ are given by;

$$\alpha(\rho_e) = \alpha_{max} - (\alpha_{max} - \alpha_{min})\rho_e^{p_\alpha} \quad (7)$$

$$\sigma_y(\lambda, \rho_e) = \sigma^0_{y,min} + (\sigma^0_{y,max} - \sigma^0_{y,min})\rho_e^{p_{\sigma y}} + HE(\rho_e)\lambda \quad (8)$$

Where $\boldsymbol{\rho_\alpha}$ and $\boldsymbol{\rho_{\sigma y}}$ are penalization factors for $\boldsymbol{\alpha}$ and $\boldsymbol{\sigma_y}$ respectively. These interpolations imply that the yield surface of one material is obtained by choosing $\boldsymbol{\rho_e} = 0$, meaning $\boldsymbol{\alpha} = \boldsymbol{\alpha_{max}}$ and $\boldsymbol{\sigma^0_y} = \boldsymbol{\sigma^0_{y, min}}$, and the second yield surface is obtained by $\boldsymbol{\rho_e} = 1$, meaning $\boldsymbol{\alpha} = \boldsymbol{\alpha_{min}}$ and $\boldsymbol{\sigma^0_y} = \boldsymbol{\sigma^0_{y, max}}$.

As above, the particular case $\boldsymbol{\alpha_{min}} = 0$ means that the plastic response of the second material is governed by the von Mises yield criterion. By setting also $\boldsymbol{\sigma^0_{y, max}} = \boldsymbol{\sigma^0_{y,steel}}$ an actual model of steel is obtained for $\boldsymbol{\rho_e} = 1$.

In Figure 1, the interpolation of the yield surfaces is demonstrated, for 2 materials resembling steel and concrete.

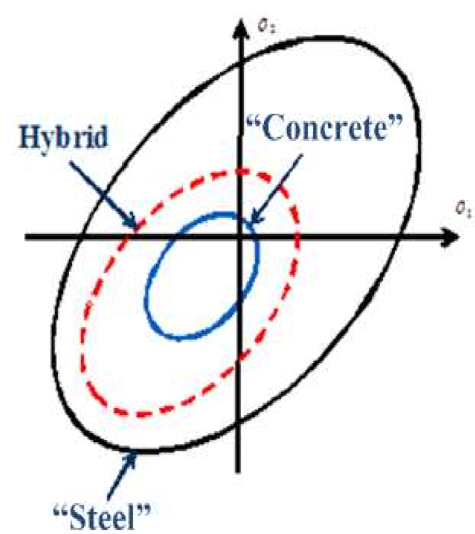

Figure 1: Demonstrative example of the interpolation between2 yield surfaces, presented in 2D principal stress space. The "Hybrid" surface represents the behavior of an artificial mixture, corresponding to an intermediate density in topology optimization.

In order to near optimal strut-and-tie designs, I extend this interpolation so it accommodates also void regions. I add another design variable **x** for each finite element. Void regions are represented by **x** = 0 and solid regions are represented by **x** = 1. Within the solid regions, the value of $\boldsymbol{\rho}$ determines the distribution of the 2 candidate materials. This leads to the following interpolation functions, replacing Eqs. **(5)**, **(6)**, **(7)**, **(8)**.

$$E(x_e,\rho_e) = x_e^{p_{Ex}}\big(E_{min} + (E_{max} - E_{min})\rho_e^{p_E}\big) \tag{9}$$

$$f(\boldsymbol{\sigma},\lambda,\rho_e,x_e) = \sqrt{3J_2} + \alpha(x_e,\rho_e)I_1 - \sigma_y(\lambda,x_e,\rho_e) = 0 \tag{10}$$

$$\alpha(x_e,\rho_e) = x_e^{p_{\alpha x}}\big(\alpha_{max} - (\alpha_{max} - \alpha_{min})\rho_e^{p_\alpha}\big) \tag{11}$$

$$\sigma_y(\lambda,x_e,\rho_e) = x_e^{p_{\sigma x}}\big(\sigma^0_{y,min} + (\sigma^0_{y,max} - \sigma^0_{y,min})\rho_e^{p_{\sigma y}} + HE(x_e,\rho_e)\lambda\big) \tag{12}$$

Where $\boldsymbol{\rho}\mathbf{E}_x$, $\boldsymbol{\rho}_{\boldsymbol{\alpha}\mathbf{x}}$ and $\boldsymbol{\rho}_{\boldsymbol{\sigma}\mathbf{x}}$ are penalization factors for **x**. In practice, one may choose to use the same penalty factors for both design variables, **x** and $\boldsymbol{\rho}$.

In this article, I focus mainly on one demonstrative class of objective functions. The aim is to find the stiffest structural layouts given certain amounts of available material. When only linear elastic response is considered, the corresponding objective is the widely used minimum compliance problem.

When nonlinear response is taken into account, one may define several different objectives that are related to the maximization of the structural stiffness. Since displacement control is preferred in the nonlinear **FE** analysis, a possible equivalent to minimizing compliance in linear elasticity is maximizing the end compliance for a given prescribed displacement. In other words, the objective is to maximize the magnitude of the load that corresponds to a certain prescribed displacement at a particular degree of freedom.

Assuming the analysis problem is solved in **N** increments, the optimization problem of distributing2 materials and void in the design domain can be stated as follows:

$$\begin{aligned}
\min_{\boldsymbol{\rho},\mathbf{x}} c(\boldsymbol{\rho},\mathbf{x}) \quad &= \quad -\theta_N \hat{\mathbf{f}}^T \mathbf{u}_N \\
\text{s.t.:} \quad & \sum_{e=1}^{N_e} v_e x_e \le V_1 \\
& \sum_{e=1}^{N_e} v_e \rho_e \le V_2 \\
& 0 < x_{min} \le x_e \le 1, \qquad e = 1,\dots,N_e \\
& 0 \le \rho_e \le 1, \qquad e = 1,\dots,N_e \\
\text{with the coupled residuals:} \quad & \mathbf{R}_n(\mathbf{v}_n,\theta_n) = 0 \qquad n = 1,\dots,N \\
& \mathbf{H}_n(\mathbf{u}_n,\mathbf{u}_{n-1},\mathbf{v}_n,\mathbf{v}_{n-1},\boldsymbol{\rho},\mathbf{x}) = 0 \qquad n = 1,\dots,N
\end{aligned} \tag{13}$$

Where $\mathbf{V_1}$ is the total available volume of material, $\mathbf{V_2}$ is the available volume of the material whose properties correspond to $\boldsymbol{\rho}_e = 1$ ($\mathbf{V_2} \le \mathbf{V_1}$) and $\mathbf{x}_{\mathbf{min}}$ is a positive lower bound used in order to avoid singularity of the stiffness matrix. The problem of distributing 2 materials with no voids can be seen as a particular case of this formulation.

As mentioned earlier, the design sensitivities are computed by the adjoin method, following the framework for transient, nonlinear coupled problems described by Michalaras et al. To the best of the author's knowledge, this is the first implementation of this framework in topology optimization of structures with material nonlinearities.

Furthermore, it is presumably the first sensitivity analysis for topology optimization of structures with material nonlinearities where no simplifying assumptions are made. The procedure for sensitivity analysis is described here only for the 2 material and void equation**(13)** since the 2-material problem can easily be deduced from it. I begin by forming the augmented objective function $\hat{\mathbf{c}}(\boldsymbol{\rho})$.

$$\begin{aligned}
\hat{c}(\boldsymbol{\rho},\mathbf{x}) \quad = \quad & -\theta_N \hat{\mathbf{f}}^T \mathbf{u}_N - \sum_{n=1}^{N} \boldsymbol{\lambda}_n^T \mathbf{R}_n(\mathbf{v}_n,\theta_n) \\
& - \sum_{n=1}^{N} \boldsymbol{\gamma}_n^T \mathbf{H}_n(\mathbf{u}_n,\mathbf{u}_{n-1},\mathbf{v}_n,\mathbf{v}_{n-1},\boldsymbol{\rho},\mathbf{x})
\end{aligned}$$

Where $\boldsymbol{\lambda}_\mathbf{n}$ and $\boldsymbol{\gamma}_\mathbf{n}$ are the adjoin vectors to be found for all increments **n= 1**, …, **N.**I assume the initial responses $\mathbf{u_0}$, $\mathbf{v_0}$do not depend on the design variables. Furthermore, it can be observed that the objective function and the nonlinear equation systems $\mathbf{R_n}$ (**n = 1**, …, **N**) do not depend explicitly on the design variables. Therefore, the explicit terms in the derivative of the augmented objective with respect to the design variables are;

$$\frac{\partial \hat{c}_{exp}}{\partial x_e} = -\sum_{n=1}^{N} \boldsymbol{\gamma}_n^T \frac{\partial \mathbf{H}_n}{\partial x_e}$$

$$\frac{\partial \hat{c}_{exp}}{\partial \rho_e} = -\sum_{n=1}^{N} \boldsymbol{\gamma}_n^T \frac{\partial \mathbf{H}_n}{\partial \rho_e}$$

The adjoin vectors **n** (**n = 1**, …, **N**) are computed on a Gauss point level by a backward incremental procedure, which is needed due to path dependency of the elastic-plastic response. The backward procedure consists of the collection of equation systems resulting from the requirement that all implicit derivatives of the design variables will vanish.

For performing the backwards-incremental sensitivity analysis, the derivatives of the global and local residuals with respect to the analysis variables are required. These are given in this section for the elastic-plastic model utilized in the current study. In particular, I consider a plane stress situation, meaning the stresses and strains are collected in a vector with 3 entries: $\boldsymbol{\alpha} = [\boldsymbol{\alpha}_{11}, \boldsymbol{\alpha}_{22}, \boldsymbol{\alpha}_{12}]^T$ and $\boldsymbol{\varepsilon} = [\boldsymbol{\varepsilon}_{11}, \boldsymbol{\varepsilon}_{22}, \boldsymbol{\varepsilon}_{12}]^{T.}$ The derivative of the global residual is independent of the specific material model employed and is given by;

$$\frac{\partial(\mathbf{R}_n)}{\partial(\mathbf{v}_n)} = \left[\begin{array}{cc} -\mathbf{B}^T wJ_{(8\times3)} & \mathbf{0}_{(8\times1)} \end{array}\right]$$

Where **B** is the standard strain-displacement matrix; **w** is the Gauss point Light for numerical integration; and **J** is the determinant of the Jacobian at the Gauss point. For the nonlinear material model described in Section **5**, the derivatives of the local residual are;

$$\begin{aligned}
\frac{\partial(\mathbf{H}_n)}{\partial(\mathbf{u}_n)} &= \left[\begin{array}{c} \mathbf{B}_{(3\times8)} \\ \mathbf{0}_{(1\times8)} \end{array}\right] \\
\frac{\partial(\mathbf{H}_{n+1})}{\partial(\mathbf{u}_n)} &= \left[\begin{array}{c} -\mathbf{B}_{(3\times8)} \\ \mathbf{0}_{(1\times8)} \end{array}\right] \\
\frac{\partial(\mathbf{H}_n)}{\partial(\mathbf{v}_n)} &= \left[\begin{array}{cc} -\mathbf{D}^{-1} - \Delta^n\lambda\frac{\partial^2 f}{\partial\boldsymbol{\sigma}_n}_{(3\times3)} & -\frac{\partial f}{\partial\boldsymbol{\sigma}_n}^T_{(3\times1)} \\ \frac{\partial f}{\partial\boldsymbol{\sigma}_n}_{(1\times3)} & -HE_{(1\times1)} \end{array}\right] \\
\frac{\partial(\mathbf{H}_{n+1})}{\partial(\mathbf{v}_n)} &= \left[\begin{array}{cc} \mathbf{D}^{-1}{}_{(3\times3)} & \frac{\partial f}{\partial\boldsymbol{\sigma}_{n+1}}^T_{(3\times1)} \\ \mathbf{0}_{(1\times3)} & 0_{(1\times1)} \end{array}\right]
\end{aligned}$$

Where the derivative of the yield function with respect to the stress components is;

$$\frac{\partial f}{\partial\boldsymbol{\sigma}} = \frac{1}{2\sqrt{3J_2}}\left[\begin{array}{ccc} 2\sigma_{11}-\sigma_{22} & 2\sigma_{22}-\sigma 11 & 6\sigma_{12} \end{array}\right] + \alpha\left[\begin{array}{ccc} 1 & 1 & 0 \end{array}\right]$$

In actual implementation, the derivatives of the local residuals $\mathbf{H_n}$ and $\mathbf{H_{n+1}}$ should maintain consistency with respect to the analysis. This means that some rows and columns should be disregarded in case of elastic loading or unloading. For example, if increment **n** is elastic, then I have $\frac{\partial(\mathbf{H_n})}{\partial(\mathbf{u_n})} = \left[\mathbf{B}_{(3\times8)}\right]$ and $\frac{\partial(\mathbf{H_n})}{\partial(\mathbf{v_n})} = \left[-\mathbf{D}^{-1}_{(3\times3)}\right]$.

Finally, computing the derivatives $\frac{\partial\mathbf{H_n}}{\partial x_e}, \frac{\partial\mathbf{H_n}}{\partial\rho_e}$ requires adding the dependency on the design variables to Eq. (4) and differentiating with respect to $\mathbf{x_e}$ and $\boldsymbol{\rho}_\mathbf{e}$. This leads to;

$$\begin{aligned}
\frac{\partial\mathbf{H}_n}{\partial x_e} &= \left[\begin{array}{c} -\frac{\partial(\mathbf{D}(x_e,\rho_e)^{-1})}{\partial x_e}(\boldsymbol{\sigma}_n - \boldsymbol{\sigma}_{n-1}) - \frac{\partial(\frac{\partial f}{\partial\boldsymbol{\sigma}_n}(x_e,\rho_e))^T}{\partial x_e}(\lambda_n - \lambda_{n-1}) \\ \frac{\partial f(x_e,\rho_e)}{\partial x_e} \end{array}\right] \\
\frac{\partial\mathbf{H}_n}{\partial\rho_e} &= \left[\begin{array}{c} -\frac{\partial(\mathbf{D}(x_e,\rho_e)^{-1})}{\partial\rho_e}(\boldsymbol{\sigma}_n - \boldsymbol{\sigma}_{n-1}) - \frac{\partial(\frac{\partial f}{\partial\boldsymbol{\sigma}_n}(x_e,\rho_e))^T}{\partial\rho_e}(\lambda_n - \lambda_{n-1}) \\ \frac{\partial f(x_e,\rho_e)}{\partial\rho_e} \end{array}\right]
\end{aligned}$$

where

$$\begin{aligned}
\frac{\partial(\mathbf{D}(x_e,\rho_e)^{-1})}{\partial x_e} &= -\frac{1}{E(x_e,\rho_e)}\frac{\partial E(x_e,\rho_e)}{\partial x_e}\mathbf{D}(x_e,\rho_e)^{-1} \\
\frac{\partial(\mathbf{D}(x_e,\rho_e)^{-1})}{\partial\rho_e} &= -\frac{1}{E(x_e,\rho_e)}\frac{\partial E(x_e,\rho_e)}{\partial\rho_e}\mathbf{D}(x_e,\rho_e)^{-1} \\
\frac{\partial(\frac{\partial f}{\partial\boldsymbol{\sigma}_n}(x_e,\rho_e))^T}{\partial x_e} &= \frac{\partial\alpha(x_e,\rho_e)}{\partial x_e}\left[\begin{array}{c} 1 \\ 1 \\ 0 \end{array}\right] \\
\frac{\partial(\frac{\partial f}{\partial\boldsymbol{\sigma}_n}(x_e,\rho_e))^T}{\partial\rho_e} &= \frac{\partial\alpha(x_e,\rho_e)}{\partial\rho_e}\left[\begin{array}{c} 1 \\ 1 \\ 0 \end{array}\right] \\
\frac{\partial f(x_e,\rho_e)}{\partial x_e} &= \frac{\partial\alpha(x_e,\rho_e)}{\partial x_e}I_1 - \frac{\partial\sigma_y(x_e,\rho_e)}{\partial x_e} \\
\frac{\partial f(x_e,\rho_e)}{\partial\rho_e} &= \frac{\partial\alpha(x_e,\rho_e)}{\partial\rho_e}I_1 - \frac{\partial\sigma_y(x_e,\rho_e)}{\partial\rho_e}
\end{aligned}$$

The above derivatives can be easily computed using the relations given in Eqs. (9), (10), (11) & (12).

Remarks regarding sensitivity analysis for displacement-controlled analysis:

The objective function utilized in the problem formulations above is appropriate for stiffness maximization only in the case of a single point load. Applying a distributed load while prescribing a single displacement poses a problem when defining a proper objective for stiffness maximization. As discussed previously, maximizing the worldwide end compliance $\theta\widehat{\mathbf{f}}_{ext}^{T}\mathbf{u}$ may result in a structure that is very stiff with respect to bearing the load at the prescribed DOF but very flexible with respect to all other loads. Therefore when a distributed load is set, the objective is defined as minimizing the end compliance $\mathbf{f}_{ext}{}^{T}\mathbf{u}$ as if the analysis is load-controlled and as if the load intensity is constant throughout the optimization. The resulting hybrid procedure combines the advantages of both load and displacement control. On the one hand, the analysis is more stable numerically and is more likely to converge when the structural layout is relatively "soft".

On the other hand, the objective is well-defined and should lead to the best worldwide stiffness with respect to all the applied loads. Practically, this can be seen as a load-controlled procedure, just that the load intensity varies throughout the design process to _t the prescribed displacement. Moreover, in the sensitivity analysis it is assumed that the solution was obtained using load control, which leads to a more straightforward computational procedure.

IV. EXAMPLES

In this part, Ishowmany results obtained when implementing the computational approach described in this article. The aim is to demonstrate the abilities and potential of our approach and to gain insight regarding implementation aspects. Therefore, as preliminary examples I consider relatively small scale 2dimensional problems with no self-Light. Extending to 3 dimensional models and incorporating more realistic loading conditions are among the goals of future work.

The examples presented point to each the distribution of concrete and steel as well as to the distribution of concrete, steel and void (13). The material parameters resemble real values corresponding to steel and concrete, see Table 1. For computing $\boldsymbol{\alpha}_{\mathbf{max}}$ and$\boldsymbol{\sigma}^{\mathbf{0}}_{\mathbf{y,\,min}}$, both corresponding to the concrete phase, it was assumed that the strength of concrete in compression is ten times higher than in tension. All test cases Ire solved using a 2D finite element mesh consisting of square, bi-linear plane stress elements.

The optimization was performed by a nonlinear optimization program based on the Method of Moving Asymptotes - MMA. In order to obtain regularized designs and to avoid checkerboard patterns, a density filter was applied.

Table 1: Material properties in all test cases

Parameter	Material	Value
E_{min}	concrete	25.0 [GPa]
E_{max}	steel	200.0 [GPa]
α_{min}	steel	0.0
α_{max}	concrete	0.818
$\sigma^0_{y,min}$	concrete	5.5 [MPa]
$\sigma^0_{y,max}$	steel	300 [MPa]
ν	both	0.3
H	both	0.01

VI. OPTIMIZED BEAMS SUBJECT TO DISTRIBUTED LOADS

In these example problems, I again address the maximum end compliance design of beams. I consider slenderer beams with loads evenly distributed along the length, see Figure **2(a)** for the setup of a simply supported beam and Figure 3(a) for the setup of a cantilevered beam.

Due to the larger length-to-height ratio, I expect bending action to be much more dominant than in the previous example. The models of the symmetric halves are discretized with **160 ×40** and **240 ×40FE** meshes respectively the volume fraction is set to **0:1** for both cases, and the load is modeled as **10** equally spaced point loads on one half of the beam.

For the simply supported beam, I apply a specific displacement directed downwards at the mid-point of the top fiber, with a magnitude of **δ = 0:005**. For the cantilevered beam, the specific displacement is at the top of the free edge and the magnitude is **δ= 0:001**.

Examining the layouts obtained with distributed loads, it can be seen that the presented procedure enables a clear distinction between tensile and compressive stresses. In the simply supported beam, steel reinforcement is placed in the bottom fiber where tensile stresses appear due to bending, and in the vicinity of concentrated forces. Near the supports, the bottom fiber reinforcement is bent upwards. This improves the structure's resistance to shear failure, which is dominant in these regions. In the cantilevered beam, the same principals are followed, so steel is added also to the top fiber above the supports. This reinforcement is bent in both directions according to the varying dominance of shear failure in comparison to bending failure.

At the end, it can be observed that small portions of steel are used also to reinforce the support regions and to a lesser extent under loading points.

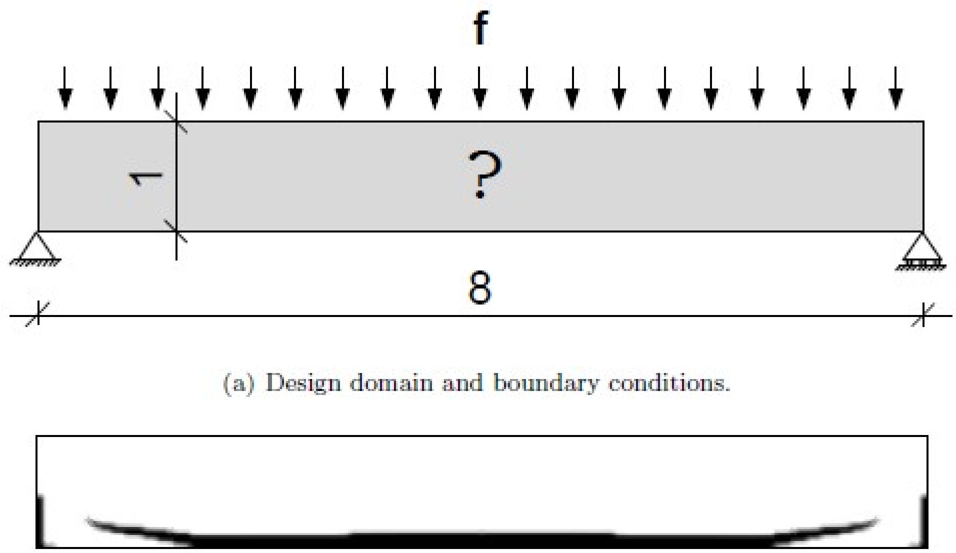

(a) Design domain and boundary conditions.

(b) Optimized layout after 150 design iterations with gradual refinement.

Figure 2: Maximum end-compliance of a simply supported beam subject to a distributed load.
Black = steel, white = concrete. Steel consists of 10% of the total volume.

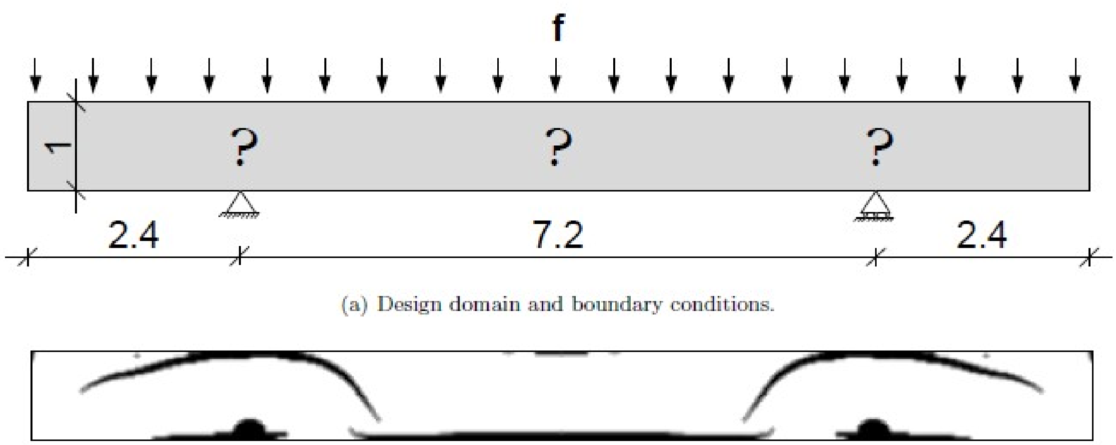

(a) Design domain and boundary conditions.

(b) Optimized layout after 300 design iterations with gradual refinement.

Figure 3: Maximum end-compliance of a cantilevered beam subject to a distributed load.
Black = steel, white = concrete. Steel consists of 10% of the total volume.

Optimized short cantilever:

In this example problem, the aimed procedure is applied for designing the reinforcement in a short cantilever. The design domain is a square supported at 2 corners on the left side and loaded with a prescribed displacement directed downwards at the opposite bottom corner. The model is discretized with a 100×100 FE mesh. The objective is to maximize the end-compliance, and Ishow2 results: one of concrete-steel distribution and another of concrete-steel-void distribution. For the 2 material design, the steel volume fraction is 0:2. When void is considered as Ill, then the total volume fraction is0:4 and the steel volume fraction is **0:1**. The specific displacements are set to **δ= 0:002** and **δ= 0:001**respectively. The penalty factors are set to the value of **3:0** and the filter radius is **r= 0:015** for all design iterations.

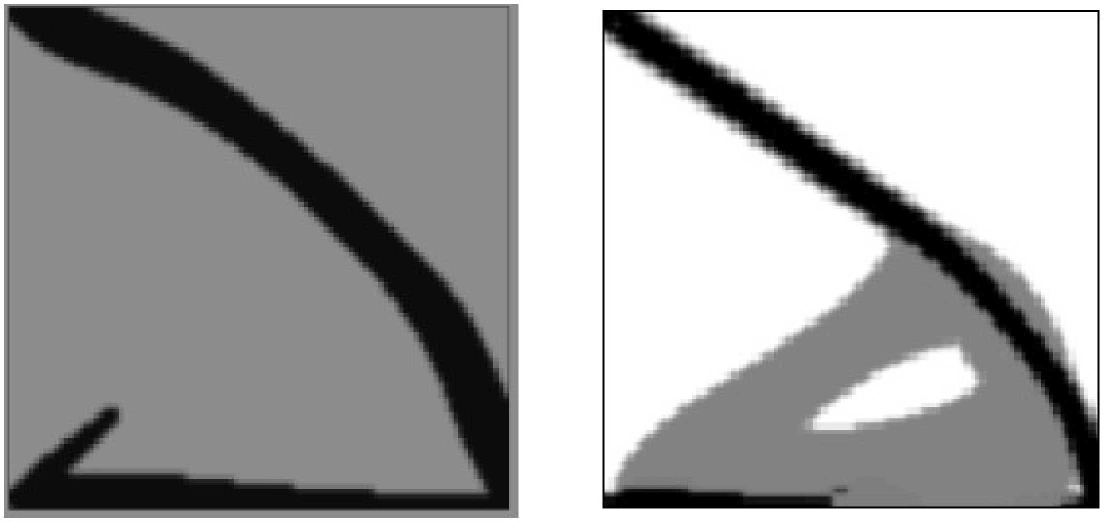

(a) Optimized layout after 500 design iterations, 80% concrete, 20% steel. Black = steel, gray = concrete.

(b) Optimized layout after 200 design iterations, 30% concrete, 10% steel, 60% void. Black = steel, gray = concrete, white = void.

Figure 4: Maximum end-compliance of a short cantilever.

In 2 cases, steel is used mainly for a cable-like member in tension, transferring the load to the upper support. This cable is then supported by either a continuous concrete domain (when no voids are possible) or by 2 compressed concrete bars, see Figures 4(a), 4(b).

This again demonstrates the ability of the process to differentiate between structural elements in tension and in compression and to select the appropriate material for each type. The layout obtained when distributing steel, concrete and void resembles strut-and-tie models that are greatly used in practical analysis and design of reinforced concrete.

As observed in previous models, steel might be used also for stiffening support regions. In the short cantilever, this is the case mainly for the 2 material problem with no voids. To a lesser extent, this is observed also in the result of the concrete-steel-void distribution.

VII. DISCUSSION

The resulting optimized layouts clearly demonstrate the potential of this approach. Once distributing steel inside a concrete beam, the location of reinforcement resembles ancient design and agrees with common engineering information. Once distributing concrete, steel and void, it's shown that optimized strut-and-tie models are generated. These may be used for many purposes: first; to supply the engineer an improved initial design before the detailed design stage. Second, to challenge ancient apply and attain a lot of economical design of reinforced concrete structures by suggesting non-traditional forms and shapes. Third, to reduce weight and concrete production, by utilizing Light weight concrete within the "void" regions where no strength is needed.

Future work can target additional realistic modeling. With reference to loading conditions, it's necessary to consider also self-weight and multiple load cases. Another vital issue is that the constraint on the amount of reinforcing material: in apply, the relative volume of steel rarely exceeds **1%**. This needs rather more refined **FE** models in which thin steel bars may be properly accomplished. Another vital extension is to consider strain softening within the concrete part. Consequently, transferring tension forces in concrete will be even less desirable, which means that a lot of realistic designs may be recommended. At the end, the introduction of alternative objective functions will be explored.

REFERENCES

[1]. M. K. Dr. Gupta and K. Sarkar, "Neural network model for the cost optimization design of a singly reinforced RCC beam," 2005.
[2]. M. Leps, "Multi-objective optimization of reinforced concrete frames," Rio de Janeiro, Brazil, 30May - 03 June 2005.
[3]. S. A. Babiker, A. M. Fathelrahman and M. E. Abdelrahman, "Design optimization of reinforced concrete beams using artificial neural network," Oct 2012.
[4]. T. Antonio and M. Pascual, Shape and size optimization of concrete shells, Cartagena, Campus Muralla del Mar: Engineering Structures, March 2010.
[5]. A. Guerra and P. D. Kiousis, "Design optimization of reinforced concrete structures," 2006.
[6]. Q. Wang, W.-l. Qiu and S.-l. Xu, "Structural optimization of steel cantilever used in concrete box girder bridge widening," Dalian University of Technology, Dalian, Liaoning China, Jun, 2015.
[7]. R. Blažek, M. Novák and P. Roun, "Scia engineer MOOT: automatic optimization of civil engineering structures," NemetschekScia, Belgium, 2005.
[8]. R. J. Balling and X. Yao, "Optimization of reinforced concrete frames," in J. Struct. Eng., ASCE, 123(2), 1997.

[9]. V. R. Rao, N. G. R. Iyengar and S. S. Rao, "Optimization of wing structures to satisfy strength and frequency requirement," 1977.
[10]. G. P. McCormick and A. V. Fiacco, "The sequential unconstrained minimization technique for nonlinear Programming Aprimal-Dual method," 1964.
[11]. N. G. R. Iyengar and S. K. Gupta, Programming methods in structural design, 1980: Edward Arnold Pub.Ltd. (UK).
[12]. R. Katarya, Optimization of multi-cellur wings under strength and vibrational constraints for simple loading, M Tech Thesis, Indian Institute of Technology, Kanpur, 1973.

AUTHOR'S BIOGRAPHIES

3rd Author

Eng. Khaled Muhammad Ali Muhammad
Ph.D. Student, Civil Engineering Dep.,
Structural Engineering Dept.,
Faculty of Engineering, Al-Azhar Univ.,
Cairo, Egypt
Born in Cairo, Egypt On 1/10/1986.
ID (EGY) No. 28610010129531
E-MAIL: eng.5aled.m.3li@gmail.com